Simple Kinetic Numerical Model Based on Rheometer Data for Ethylene–Propylene–Diene Monomer Accelerated Sulfur Crosslinking

G. Milani,[1] F. Milani[2]

[1]*Politecnico di Milano, Piazza Leonardo da Vinci 32, 20133 Milano, Italy*
[2]*CHEM.CO, Via J. F. Kennedy 2, 45030 Occhiobello, Rovigo, Italy*

Received 24 February 2011; accepted 7 May 2011
DOI 10.1002/app.34867
Published online 4 October 2011 in Wiley Online Library (wileyonlinelibrary.com).

ABSTRACT: A simple numerical model for the interpretation of the reaction kinetics in ethylene–propylene–diene monomer (EPDM) vulcanized with accelerated sulfur is presented. The model is based on the assumption that during vulcanization, a number of partial reactions occurs, both in series and in parallel, which determine the formation of intermediate compounds, including activated and matured polymers. Once written a standard first-order differential equation (DIFF-EQ) for each partial reaction, an ordinary DIFF-EQ system (ODEs), was obtained and solved through Runge–Kutta algorithms. Alternatively and more efficiently, a single second-order nonhomogenous DIFF-EQ with constant coefficients was deduced, for which a closed-form solution was derived, provided that the nonhomogenous term was approximated with an exponential function. Kinetic constants were evaluated through experimental data fitting on standard rheometer tests. To assess model predictions, an experimental campaign at different temperatures on two EPDM compounds was performed. They exhibited moderate reversion at intermediate and high curing temperatures. A nonlinear least-squares fitting was performed to evaluate unknown constants entering into the DIFF-EQ model proposed. Scaled rheometer curves fit rather well, also in the presence of reversion. In addition, partial reaction kinetic constants were provided: this gave an interesting insight into the different reticulation processes occurring during vulcanization. © 2011 Wiley Periodicals, Inc. J Appl Polym Sci 124: 311–324, 2012

Key words: computer modeling; curing of polymers; kinetics (polym.); rubber; vulcanization

INTRODUCTION

Sulfur vulcanization is the most practical method for bringing about the drastic property changes described by the term *vulcanization*, not only in natural rubber but also in the diene synthetic elastomers, such as Styrene-Butadiene Rubber (SBR), butyl, nitrile, and ethylene–propylene–diene monomer (EPDM) rubbers.

Vulcanization may be defined as any treatment that decreases the flow of an elastomer and increases its tensile strength and modulus but preserves its extensibility. Elemental sulfur is the predominant vulcanizing agent for general-purpose rubbers. It is used in combination with one or more accelerators and an activator system comprising zinc oxide and a fatty acid (normally stearic acid). The most popular accelerators are delayed-action sulfenamides, thiazoles, thiuram sulfides, dithocarbamates, and guanidines. Part or all of the sulfur may be replaced by a sulfur donor, such as a thiuram disulfide.

Despite the great diffusion and popularity of such kinds of vulcanization processes, probably related to the fact that sulfur is the most economical method for vulcanizing natural rubber, all of the dienic family rubbers and EPDM elastomers, its chemistry of vulcanization is somewhat complex and has not been well understood for the more than a century of practice of the process, since its discovery by Goodyear in 1839.[1–3] With a focus exclusively on EPDM rubber, because of the prohibitive complexity of the reactions induced by sulfur during crosslinking, in contrast to peroxidic curing, no precise reaction kinetics formulas are available in the technical literature. However, for EPDM, the basic reactions involved (Fig. 1) are commonly accepted[4–7] to be the following:

$$\begin{aligned}
&\text{(a)}\ \mathrm{P} + \mathrm{A} \xrightarrow[}{K_1} \mathrm{P}_1^* \\
&\text{(b)}\ \mathrm{P}_1^* \xrightarrow[}{K_2} \mathrm{P}_\mathrm{v} \\
&\text{(c)}\ \mathrm{P}_\mathrm{v} \xrightarrow[}{K_3} \mathrm{Q}_\mathrm{x} \\
&\text{(d)}\ \mathrm{P}_\mathrm{v} \xrightarrow[}{K_4} \mathrm{D}_\mathrm{e} \\
&\text{(e)}\ \mathrm{P}_\mathrm{v} \xrightarrow[}{K_5} \mathrm{P}_{\mathrm{v}_\mathrm{f}}
\end{aligned} \qquad (1)$$

Correspondence to: G. Milani (gabriele.milani@polimi.it).

The authors wish to dedicate this work to the memory of their long-time friend and colleague Domenico Lori, who suddenly passed away.

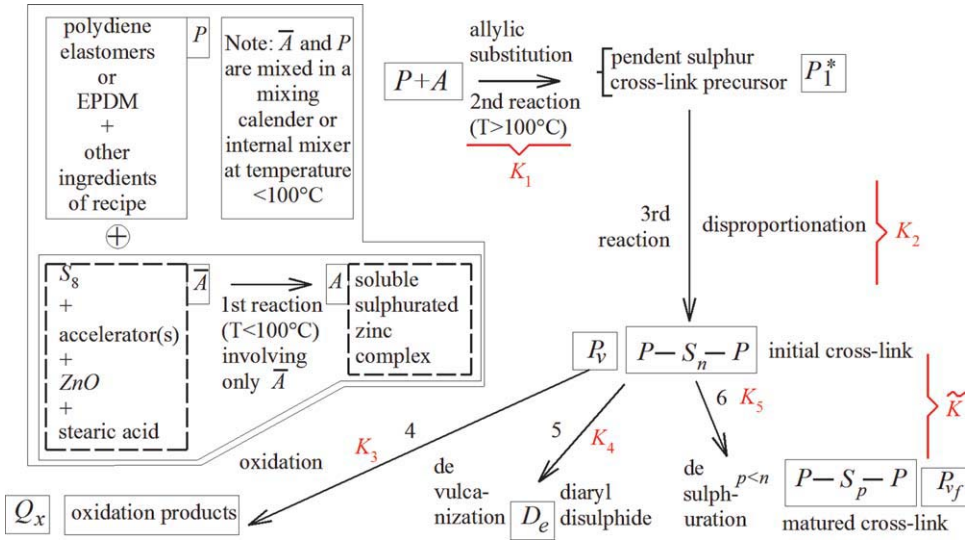

Figure 1 Products and schematic reaction mechanisms of the accelerated sulfur vulcanization of EPDM elastomers. n and p are the S atoms between the backbone of the macromolecules ($n > p$) [Color figure can be viewed in the online issue, which is available at wileyonlinelibrary.com.]

where P and A are the polymer (EPDM) and soluble sulfureted zinc complex (S_8 + Accelerators + ZnO + Stearic acid), respectively; P_1* is the pendent sulfur (crosslink precursor); P_v is the reticulated ethylene–propylene–diene monomer; P_{v_f}, Q_x, and D_e are the matured crosslink, the oxidation product, and diaryl–disulfide, respectively; and K_1–K_5 are the kinetic reaction constants, which depend only on the reaction temperature.

Here, it is worth noting that eq. (1a) represents the allylic substitution in Figure 1, eq. (1b) is the disproportionation, and eqs. (3c)–(3e), occurring in parallel, are the oxidation, desulfuration, and devulcanization, respectively.

To gain precise insight into the sulfur vulcanization kinetic, in the absence of standard chemical reaction kinetics, it is our opinion that the rheometer curve, repeated at different external curing temperatures, is the best way to gain quantitative information on the crosslinking density obtained[8] at different temperatures and curing times for sulfur vulcanization, correlated between the network structure and elastic and dynamic properties of the item. The higher the number of curves collected is, the more precise the database is describing the curing behavior at different temperatures of the compound analyzed.

In this context, the aim of the work presented here was to propose a combined experimental and numerical procedure for the interpretation of the accelerated sulfur curing and to predict any single intermediate reaction velocity and amount. To validate the numerical data obtained with the model proposed, an experimental campaign at different temperatures on two different EPDM compounds was performed. Both compounds exhibited moderate eversion at intermediate and high curing temperatures.

The mixed experimental/numerical approach proposed relies on the following blocks:

1. For a given rubber compound, rheometer curves are experimentally evaluated at different vulcanization temperatures, ranging from low to high. The curves are obtained through a rotorless rheometer according to the procedure described in the ASTM D 5289.[9]
2. The numerical model is based on the assumption that during vulcanization, the partial reactions shown in eq. (1) occur, both in series and in parallel. They determine the formation of intermediate compounds, including activated and matured polymers. Once the partial reaction constants are known, a numerical estimation of the degree of crosslinking is possible. For each partial reaction, standard first-order differential equations (DIFF-EQs) are written, and a first-order DIFF-EQ system is obtained [ordinary differential equation (ODE) system], which can be solved with numerically expensive Runge–Kutta algorithms. Alternatively and more efficiently, a single second-order nonhomogenous DIFF-EQ with constant coefficients is derived in the article, for which a solution may be found in closed form, provided that the nonhomogenous term is approximated with an exponential function.
3. To provide an estimation of the degree of vulcanization of the cured EPDM, kinetic model constants are estimated through a nonlinear

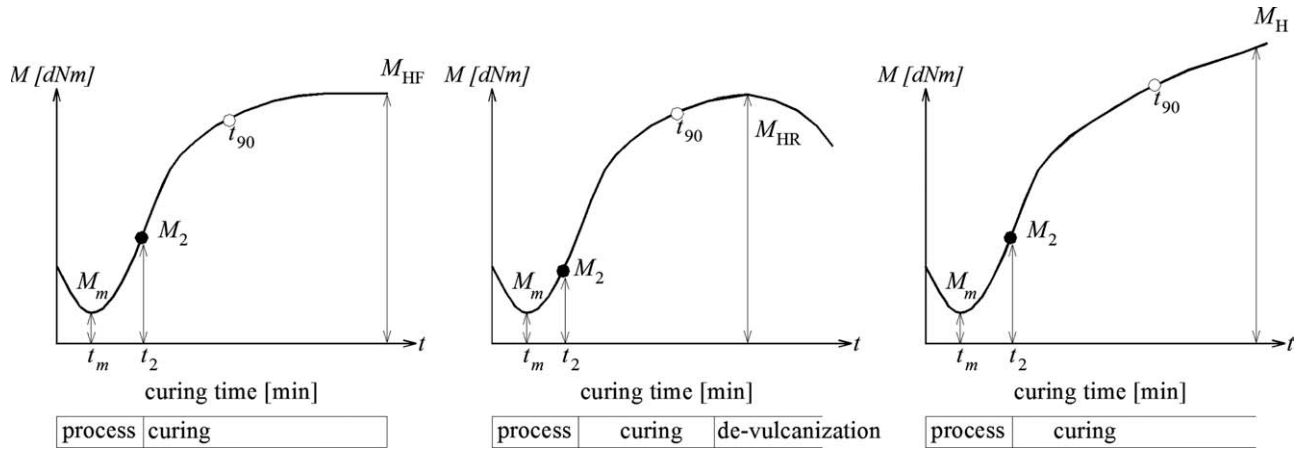

Figure 2 Typical experimental behavior of a rubber compound during rheometer testing. M is the torque, M_{HF} is the maximum torque where the curve plateaus, M_{HR} is the maximum torque of reverting curve, M_H is the highest torque attained during a specified period of time when no plateau or maximum torque is obtained.

least-squares fitting of the numerical data, on standard rheometer experimental tests available from the experimental campaign. The procedure is based on an interior-reflective Newton method, which allows one to quickly evaluate unknown constants entering into the DIFF-EQ model proposed. The experimental campaign is performed at different temperatures on two different EPDM commercial compounds. Both of them exhibit reversion at intermediate and high curing temperatures.

From these considerations, it is worth noting that the approach proposed here is somewhat different with respect to previously presented models suitable for the analysis of natural rubber (see Ding and Leonov[10]) and rubber cured with peroxides.[7,11,12] Although for natural rubber, reactions are different and a rather approximate numerical model was proposed in Ding and Leonov,[10,13] in the latter case, the kinetic reaction to consider is a single one, following Arrhenius law.[12,14] For EPDM sulfur vulcanization, the reaction kinetics are much more intricate and require an experimental characterization of the compound itself.

VULCANIZATION OF EPDM WITH ACCELERATED SULFUR. EXPERIMENTAL CAMPAIGN: POLYMERS USED, BLENDS, AND RHEOMETER CURVES

Sulfur vulcanization of natural rubber was discovered more than 150 years ago; however, its reaction mechanism is still not completely understood. For this reason, in what follows, we focus on combining a probable vulcanization kinetic scheme particularly suited to EPDM rubber[4,7] with experimental cure curves obtained with a RPA 2000 rubber processing analyzer (Polimeri Europa, Ferrara, Italy) rheometer, following the ASTM D 5289[9] method.

In more detail, it is commonly accepted that the variation of the cure-meter curve (Fig. 2), intended as the progressive increase of stiffness during vulcanization, macroscopically characterizes the rubber reticulation level. Cure-meter torque values are here correlated with the reticulation kinetic parameters, deduced by a numerical and analytical approach based on the assumption of a sequence of elementary reactions occurring both in series and in parallel, each one represented quantitatively by a first-order differential kinetic. As mentioned, the polymers considered all belonged to the family of EPDMs, where it was expected that the mechanism at the base of vulcanization was similar to that generally accepted for polydiene elastomers.[15,16]

In the case of EPDM, accelerated sulfur vulcanization resulted in the substitution of the labile allylic H atoms by sulfur bridges to yield alkenyl suphides.[17–20]

Even though EPDM may be obtained with different diene monomers, for instance, ethyldiene norbornene (ENB), vinyl norbornene, and dicyclopentadiene, here attention was focused on ENB only because all of the EPDM compounds analyzed experimentally in the study were obtained from ENB.

Pendent ENB unsaturation is not consumed but activates the allylic positions via a sulfur bridge to yield crosslinking precursors. Subsequently, actual sulfur crosslinks are formed. Sulfur substitution of ENB occurs at C-3 exo, C-3 endo, and C-9 (not at bridge head C-1). At elevated temperatures, desulfuration occurs; this results in the formation of shorter sulfur bridges.[21] Side reactions, such as cis–trans isomerization, allylic rearrangement, and/or the formation of conjugated dienes and trienes, are frequently observed for polydiene elastomers but do not occur during the vulcanization of EPDM containing ENB because of the stability of the *tris*-alkyl substituted unsaturation in ENB and its isolation from other ENB units in the macromolecules. In

TABLE I
Different EPDMs Analyzed Experimentally

	Type of EPDM by Polimeri Europa		
	Dutral 9046	Dutral 4049	Dutral 4044
Propylene (wt %)	31	40	35
ENB (wt %)	9.0	4.5	4.0
ML(1 + 4) 100°C	67	93	44
ML(1 + 4) 125°C	49	76	32

particular, because of the double bond outside the macromolecular chain of the backbone, a very high stability, both at high temperatures and in the presence of oxidizing agents, is expected. The formation of carbonyls at C-5 and/or C-8 of ENB–EPDM due to oxidation was shown to be linked to the accelerated sulfur vulcanization of EPDM.[22] To summarize, with all of the vulcanization issues previously pointed out taken into consideration, the basic reaction scheme represented in Figure 1 can be adopted. Each single elementary reaction is considered to be contemporary with the others, and the overall reticulation occurring during vulcanization (matured polymer concentration) is linked to rheometer cure curves, to derive numerically standard chemical reaction kinetic constants.

The vulcanization characteristics of vulcanizable rubber compounds is experimentally determined by means of a rotorless cure meter (ASTM D 5289[9]). Rotorless cure meters were introduced in the 1980s. These instruments have been replacing the oscillating disc variety because of their faster temperature recovery, improved test sensitivity, and better precision. The method permits one to measure not only the scorch time (t_2) but also the variation of the stiffness (a measure of torque) value as a function of time, continuously and during the entire vulcanization process, thus recording the whole cure curve.

All of the specimens are directly loaded between the dies maintained at a fixed temperature. The output information provided experimentally is the torque (measured in tenths of newton meters) as a function of the curing time. Such a curve obviously changes with the variation of the external curing temperature. With reference to the cure curves depicted in Figure 2, t_2 is defined as the time to incipient cure and mathematically represents the point at which the second derivative of the rheometer curve is equal to zero. A torque equal to M_2 was reached at a corresponding t_2. t_{90} and t_{100} in the cure curve are the approximate times at which 90% of crosslinking occurred and the time at which the cure curve reached its maximum torque value (M_{HF}: maximum torque where the curve plateaus), respectively. Finally, it is interesting to notice that the cure curve also exhibits a minimum point (coordinates: t_m, M_m), reached quickly during the experimentation in the rheometer. However, such an initial part of the cure curve is of very little importance for the prediction of the final reticulation level. For this reason, it was intentionally not included in the DIFFEQ model adopted in the article, compare, for instance, the system in eq. (1) and Figure 1.

Two different EPDMs were experimentally tested in this work. Some supplementary data for a further compound (Dutral TER 4044) were also considered, for which experimentation is still running at the time of this writing. The characteristics of these EPDMs, in terms of Mooney viscosity and compositions, are summarized in Table I.

For all types of EPDM considered in this work, the same formulation was used, with the precise aim of comparing the polymeric matrix in the presence of different Mooney viscosities and different ENB contents but with a composition where the elastomers were completely in an amorphous state. In Table II, the compounds formulation adopted (in parts per hundred resin) is summarized.

The vulcanization was carried out in an autoclave with a discontinuous system to control as well as possible the vulcanization conditions, in particular, the temperature uniformity and time. Previously, we prepared the compounds in an internal mixer (Polimeri Europa, Ferrara, Italy); we added both curing and accelerating agents to the roll mixer, starting at room temperature and maintaining it under 100°C for all the time of the operation. Then, each sample was analyzed with a rotorless cure meter, following specifics provided for RPA 2000. A rubber process analyzer (RPA 2000) was used instead of a moving die rheometer because of its ability to follow the material behavior before, during, and after cure.

Generally, the tests were performed at three different temperatures (160, 180, and 200°C), except for Dutral 9046, for which the test at 200°C was not performed because reversion was registered just at 180°C. The resultant experimental cure curves for Dutral 4049 and Dutral 9046 are represented in Figures 3 and 4, respectively. Furthermore, in Figure 5, the experimental cure curves for Dutral 4049 and Dutral 9046 are compared at 160 and 180°, respectively. As can be noted, there were some perceivable differences between the compounds analyzed only at 180°. In particular, it is worth mentioning here

TABLE II
Compound Formulation Adopted (phr)

Ingredient	Description	phr
Polymer	Dutral 4049, 9046, and 4044	100
Zinc oxide	Activator	5
Stearic acid	Coagent	1
HAFN 330	Carbon black	80
Paraffinic oil	Wax	50
Sulfur	Vulcanization agent	1.5
TMTD	Tetramethylthiuram disulfide	1.0
MBT	Mercaptobenzothiazole	0.5

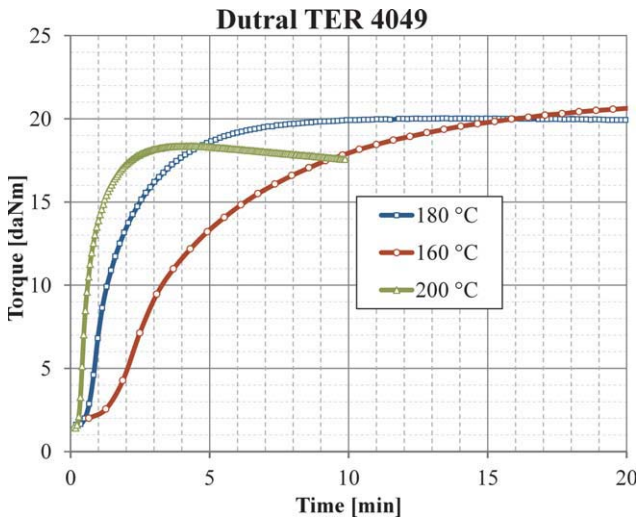

Figure 3 Experimental rheometer curves of Dutral TER 4049 at 160, 180, and 200°C. [Color figure can be viewed in the online issue, which is available at wileyonlinelibrary. com.]

that the first compound (Dutral 4049) was an EPDM with a small percentage of ENB, whereas the second (Dutral 9046) had a high ENB content. As expected, the compound with the high ENB content exhibited reversion at high–medium vulcanization temperatures (e.g., 180°C); this indicates that a devulcanization occurred.

Here, it is worth noting that in the industrial production of terpolymers 4049 and 4044, as in Table I, vulcanization is usually performed at 160, 180, and 200°C for 60, 20, and 4.5 min. For Dutral 9046, the curing time at 160°C was 30 min, and that at 180° was 4.5 min.

Although the kinetic mathematical model proposed in the following section was calibrated exclusively on RPA 2000 experimental rheometer curves, for the sake of completeness, a mechanical experimental characterization of the compounds in uniaxial tension was also conducted to gain insight into the stress–stretch behavior of small samples in the presence or absence of insaturation.

It has to be emphasized that in practice, the tensile strength, modulus, and elongation at break are evaluated on specimens with the maximum possible vulcanization level, a condition corresponding to ending the curing process immediately after t_{100}. In the presence of reversion, it does not correspond to the end-of-test instant. Therefore, the mechanical characterization hereafter presented refers to specimens with a vulcanization level corresponding to the maximum torque.

The tensile strength, elongation, and modulus values obtained for vulcanized items were the mean

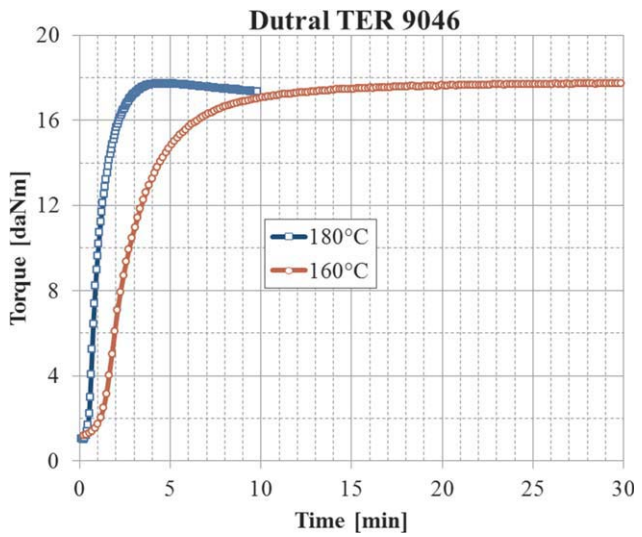

Figure 4 Experimental rheometer curves of Dutral TER 9046 at 160 and 180°C. [Color figure can be viewed in the online issue, which is available at wileyonlinelibrary.com.]

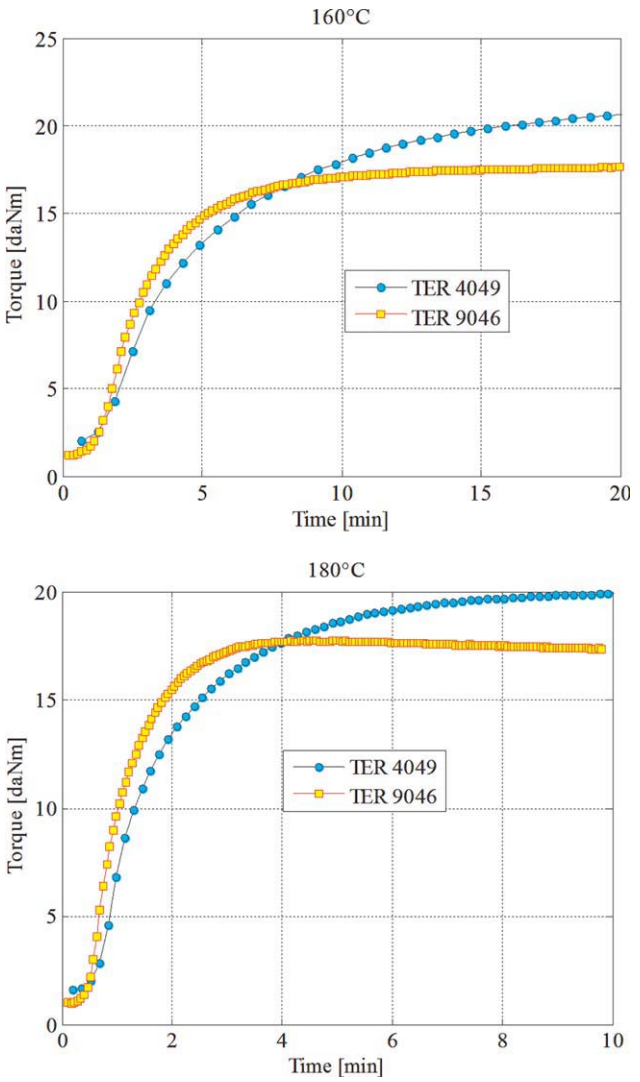

Figure 5 Comparison between the experimental cure curves of Dutral TER 4049 and TER 9046 at 160 and 180°C. [Color figure can be viewed in the online issue, which is available at wileyonlinelibrary.com.]

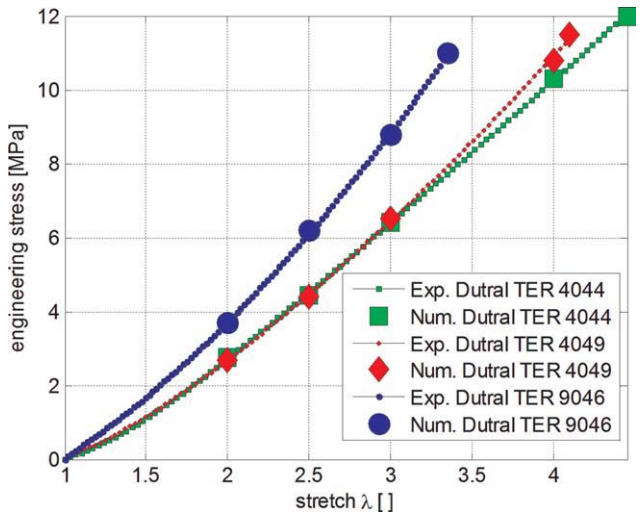

Figure 6 Comparison among the experimental stretch–stress curves for Dutral TER 4044, 4049, and 9046. The continuous lines are numerical extrapolations of the experimental data (■, ◆, and ●) obtained with a five-constant Mooney–Rivlin model. [Color figure can be viewed in the online issue, which is available at wileyonlinelibrary.com.]

values of the experimental data obtained by the testing of rubber specimens vulcanized at the different temperatures considered,[23,24] that is, 160, 180, and 200°C for Dutral 4049 and 4044 and 160 and 180°C for Dutral 9046.

As can be noted from the stretch–stress diagrams depicted in Figure 6, the influence of the ENB amount in the polymer was remarkable. Indeed, the two polymers with a lower amount of ENB and very different Mooney viscosities, that is, Dutral 4044 and 4049, had quite similar behavior in terms of the modulus and stress–strain at break. In the case of Dutral 9046, an increase in modulus with a decrease of elongation at break was observed. This means that an increase of cure density was obtained with increasing ENB in the polymer. As already pointed out, the crosslinking process through sulfur and accelerators is an also extremely complex process in the case of EPDM. However, if a sufficiently refined numerical model is used, an estimation of the double-bond density may be attempted and thus, ENB may be dosed in a programmable quantity.

In conventional vulcanization, crosslinkage is introduced in considerable excess with respect to the number of primary (linear) macromolecules. Ordinarily, a repeating module ranging from 50 to 100 units is crosslinked. Because the primary molecules may range from 1000 to 2000 units, an average of 10–40 crosslinked units per primary molecule is normally expected.[25] For the compounds at hand, in the presence of one double bond and two double bonds percentage molar in the macromolecules, the deduction of kinetic parameters through contemporary elementary reactions seemed reasonable, and it was expected that the *a priori* evaluation of the cure density and of the mechanical characteristics of vulcanized compounds would be in agreement with the experimental evidence.

PROPOSED KINETIC MATHEMATICAL MODEL

The chemical reactions occurring during sulfur vulcanization reported in eq. (1) obey the following rate equations:

$$\begin{aligned}
\frac{dP}{dt} &= -K_1AP \\
\frac{dP_v}{dt} &= K_2P_1^* - K_3Q_x - K_4D_e - K_5P_{v_f} \\
\frac{dQ_x}{dt} &= K_3P_v \\
\frac{dD_e}{dt} &= K_4P_v \\
\frac{dP_{v_f}}{dt} &= K_5P_v
\end{aligned} \tag{2}$$

By means of the so-called *xyz* method, independent variables may be established.

From the stoichiometry of the reaction, it can be argued that

$$\begin{aligned}
A &= A_0 - x \\
P &= P_0 - x \\
P_1^* &= x - y = (P_0 - P) - y \\
&= (P_0 - P) - \left(P_v + Q_x + D_e + P_{v_f}\right) \\
P_v &= y - z - q - r \\
Q_x &= z \\
D_e &= q \\
P_{v_f} &= r
\end{aligned} \tag{3}$$

where A_0 and P_0 are the initial concentration of curing agent and polymer respectively.

Obviously, from eq. (3), it can be argued that the independent variables are $P(t)$, $P_v(t)$, $Q_x(t)$, $D_e(t)$, with t time variable and P_{v_f}. The aim is to provide an analytical expression for vulcanized rubber, that is, the concentration of $P_v(t)$ with respect to time.

From eqs. (2) and (3), the following set of DIFFEQs is deduced:

$$\begin{aligned}
&\text{(a)}\ \frac{dP}{dt} = -K_1AP \\
&\text{(b)}\ \frac{dP_v}{dt} = K_2P_1^* - K_3Q_x - K_4D_e - K_5P_{v_f} \\
&\qquad = K_2\left[(P_0 - P) - \left(P_v + Q_x + D_e + P_{v_f}\right)\right] \\
&\qquad\quad -K_3Q_x - K_4D_e - K_5P_{v_f} \\
&\text{(c)}\ \frac{dQ_x}{dt} = K_3P_v \\
&\text{(d)}\ \frac{dD_e}{dt} = K_4P_v \\
&\text{(e)}\ \frac{dP_{v_f}}{dt} = K_5P_v
\end{aligned} \tag{4}$$

Obviously the first-order DIFF-EQ system in eq. (4) can be solved with a standard Runge–Kutta numerical approach.[26] However, such a procedure, when coupled with a nonlinear least-squares algorithm (as in the case here), may become excessively slow (especially for stiff problems) and, in some cases, may fail to converge to experimental data fitting. Here, an alternative procedure was envisaged, which used a single DIFF-EQ, for which an analytical solution could be found. With an analytical expression for the crosslinked polymer concentration at our disposal, a least-squares numerical fitting was much more efficient, and numerical failures were circumvented.

In more detail, differentiating eq. (4b) with respect to time, we obtain

$$\frac{d^2P_v}{dt^2} = -K_2\left(\frac{dP}{dt} + \frac{dP_v}{dt} + \frac{dQ_x}{dt} + \frac{dD_e}{dt} + \frac{dP_{v_f}}{dt}\right) - K_3\frac{dQ_x}{dt} - K_4\frac{dD_e}{dt} - K_5\frac{dP_{v_f}}{dt} \quad (5)$$

Considering also the relations reported in eqs. (4) and (5), we could rewrite this as follows:

$$\frac{d^2P_v}{dt^2} + K_2\frac{dP_v}{dt} + \tilde{K}^2P_v = -K_2\frac{dP}{dt} = K_1K_2AP \quad (6)$$

The following constant is indicated by $\tilde{K}^2$:

$$\tilde{K}^2 = K_2(K_3 + K_4 + K_5) + K_3^2 + K_4^2 + K_5^2 \quad (7)$$

Assuming that moles of $A = P$, as the stoichiometry of the reaction[27] suggests, we could write that

$$\frac{dP}{dt} = -K_1AP \qquad \frac{dA}{dt} = -K_1AP \quad (8)$$

Hence, $P_0 - P = A_0 - A$ [see also eq. (8)], and if $P_0 = A_0$, eq. (5) becomes

$$\frac{dP}{dt} = -K_1P^2 \quad (9)$$

This is a first-order DIFF-EQ with separable variables. For eq. (9), the definite integral is

$$-\frac{1}{P(t)} + \frac{1}{P_0} = -K_1t \Rightarrow P(t)P_0K_1t = P_0 - P(t) \Rightarrow P(t) = \frac{P_0}{(P_0K_1t + 1)} \quad (10)$$

Substituting the explicit solution for $P(t)$ [eq. (10)] into eq. (6), we obtain the following DIFF-EQ:

$$\frac{d^2P_v}{dt^2} + K_2\frac{dP_v}{dt} + \tilde{K}^2P_v = -K_2\frac{dP}{dt} = \frac{K_1K_2P_0^2}{(P_0K_1t + 1)^2} \quad (11)$$

This is a nonhomogenous second-order DIFF-EQ with constant coefficients. To determine the analytical expression of the function $P_v(t)$, the solution of the associated homogeneous DIFF-EQs and a particular integral has to be found.

The determination of integrals of the homogeneous equation corresponding to the left hand side of eq. (11) is trivial and can be achieved by consideration of the roots ($\lambda_{1,2}$) of the characteristic polynomial:

$$\lambda^2 + K_2\lambda + \tilde{K}^2 = 0 \quad (12)$$

which are

$$\lambda_{1,2} = \frac{-K_2 \pm \sqrt{K_2^2 - 4\tilde{K}^2}}{2} = \alpha \pm \beta \quad (13)$$

where $\alpha = -\frac{1}{2}K_2$ and $\beta = \sqrt{(K_2/2)^2 - \tilde{K}^2}$. From obvious physical considerations, it could be argued that $K_2 \gg K_3 \approx K_4 \approx K_5$ and, hence, $K_2/2 > \tilde{K}$, which means that $(K_2/2)^2 - \tilde{K}^2 > 0$.

In this case, the solution of the homogeneous DIFF-EQ corresponding to eq. (6) is

$$P_v(t) = C_1e^{(\alpha+\beta)t} + C_2e^{(\alpha-\beta)t} \quad (14)$$

where C_1 and C_2 are two constants that can be determined from the initial conditions.

The determination of the particular integral of eq. (11) is not an easy task. Indeed, to find a particular integral for function $g(t)$, where

$$g(t) = \frac{1}{(P_0K_1t + 1)^2} \quad (15)$$

is nontrivial.

In the absence of consolidate *ad hoc* procedures, the so-called general technique of the variation of the arbitrary constants should be used. However, such a general procedure provides only the first derivatives of some functions entering into the particular integral, and their analytical integration is, in any case, not possible. Here, an alternative procedure is proposed, which consists of substitution of the original function $g(t)$, which represents (apart from multiplying constants) the right hand side of eq. (11), with a fitting function $f(t)$ in the following form:

$$f(t) = \gamma_1e^{\gamma_2K_1P_ot} \quad (16)$$

where γ_1 and γ_2 are constants to be further determined in such a way that eq. (16) fits as close as possible [eq. (15)].

Equation (16) has the rather important advantage that it is an exponential function, for which a particular integral is at one's disposal.

To make eq. (16) near to the original function [eq. (15)], we require that

$$f(0) = g(0)$$
$$\int_0^{t_m\to\infty} f(t)dt = \int_0^{t_m\to\infty} g(t)dt \tag{17}$$

Here, it is worth noting that the first request means that functions have the same initial value, whereas the second imposes that the average decay of nonpolymerized reagent is the same, with the implicitly accepted simplifying hypothesis that at the end of the test (in practice for an infinite time), the nonpolymerized reagent is negligible.

From eq. (17), we obtain that

$$\gamma_1 = 1 - \frac{1}{K_1P_0}\frac{1}{K_1P_0t+1}\Big|_0^\infty = -\frac{1}{\gamma_2K_1P_0}e^{-\gamma_2K_1P_0t}\Big|_0^\infty$$
$$\Rightarrow \gamma_2 = 1 \tag{18}$$

From eq. (18), the nonhomogenous differential eq. (11) can be rewritten as follows:

$$\frac{d^2P_v}{dt^2} + K_2\frac{dP_v}{dt} + \tilde{K}^2P_v = K_1K_2P_0^2e^{-K_1P_0t} \tag{19}$$

For eq. (19), the determination of a particular integral is trivial. It is

$$P_v^p(t) = K_1K_2P_0^2\left[(K_1P_0)^2 - K_2(K_1P_0) + \tilde{K}^2\right]^{-1}e^{-K_1P_0t} \tag{20}$$

where $P_v^p(t)$ indicates the particular integral.

Hence, from eqs. (19) and (14), the solution of the DIFF-EQ is

$$P_v(t) = C_1e^{(\alpha+\beta)t} + C_2e^{(\alpha-\beta)t} + K_1K_2P_0^2\left[(K_1P_0)^2 - K_2(K_1P_0) + \tilde{K}^2\right]^{-1}e^{-K_1P_0t} \tag{21}$$

with the first derivative

$$\frac{dP_v(t)}{dt} = (\alpha+\beta)C_1e^{(\alpha+\beta)t} + (\alpha-\beta)C_2e^{(\alpha-\beta)t} - K_1^2K_2P_0^3\left[(K_1P_0)^2 - K_2(K_1P_0) + \tilde{K}^2\right]^{-1}e^{-K_1P_0t} \tag{22}$$

To fully solve the problem, it is necessary to determine C_1 and C_2. They are found from the initial conditions:

$$P_v(0) = 0$$
$$\left.\frac{dP_v}{dt}\right|_{t=0} = K_2P^*(0) = 0 \tag{23}$$

Equation (23) leads to the following linear system of equations:

$$\begin{cases} C_1 + C_2 = -\rho \\ (\alpha+\beta)C_1 + (\alpha-\beta)C_2 = K_1P_0\rho \end{cases} \Rightarrow$$
$$\begin{cases} C_2 = -\rho - C_1 \\ 2\beta C_1 = (K_1P_0 + \alpha - \beta)\rho \end{cases} \Rightarrow \begin{cases} C_2 = \rho\left(-\frac{K_1P_0}{2\beta} - \frac{\alpha}{2\beta} - \frac{1}{2}\right) \\ C_1 = \rho\left(\frac{K_1P_0}{2\beta} + \frac{\alpha}{2\beta} - \frac{1}{2}\right) \end{cases} \tag{24}$$

with ρ equal to $K_1K_2P_0^2[(K_1P_0)^2 - K_2(K_1P_0) + \tilde{K}^2]^{-1}$. To summarize, the EPDM degree of vulcanization turns out to obey in the model the following equation:

$$P_v(t) = C_1e^{(\alpha+\beta)t} + C_2e^{(\alpha-\beta)t} + \rho e^{-K_1P_0t} \times \begin{cases} C_2 = \rho\left(-\frac{K_1P_0}{2\beta} - \frac{\alpha}{2\beta} - \frac{1}{2}\right) \\ C_1 = \rho\left(\frac{K_1P_0}{2\beta} + \frac{\alpha}{2\beta} - \frac{1}{2}\right) \\ \rho = K_1K_2P_0^2\left[(K_1P_0)^2 - K_2(K_1P_0) + \tilde{K}^2\right]^{-1} \\ \alpha = -\frac{K_2}{2} \\ \beta = \sqrt{(K_2/2)^2 - \tilde{K}^2} \\ \tilde{K}^2 = \tilde{K}^2 = K_2(K_3 + K_4 + K_5) + K_3^2 + K_4^2 + K_5^2 \end{cases} \tag{25}$$

The kinetic constants that need to be determined are only three, that is, K_1, K_2, and $\tilde{K}^2$.

The most straightforward method for numerically estimating the kinetic constants is to fit eq. (25) onto the experimental cure curve by normalized scaling of the peak value to P_0 and translating the initial rotation resistance to zero, as suggested by Ding and Leonov.[10]

As a rule, variables K_1, K_2, and $\tilde{K}^2$ are estimated through a standard nonlinear least-squares routine. Because the problem is rather easy to handle, a trust-region-reflective algorithm is used. This algorithm is a subspace trust-region method and is based on the interior-reflective Newton method.[28,29] Each iteration involves the approximate solution of a linear system with the method of preconditioned conjugate gradients.

To summarize, two numerical models have been discussed. The first relies on a system of first-order DIFF-EQs [eq. (4)], which represent an ODE system, whereas the second is a single second-order nonhomogenous DIFF-EQ with constant coefficients

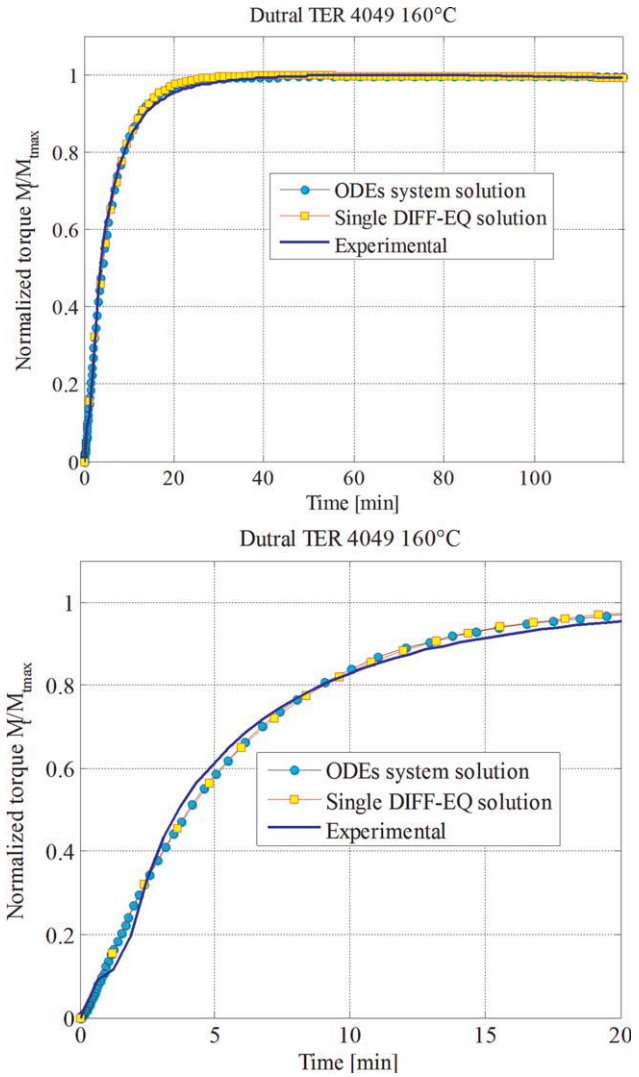

Figure 7 Comparison between the experimental data and the numerical models proposed (bottom: detail at initial vulcanization instants) for Dutral TER 4049 at 160°C. M_{max} is the maximum torque during experimentation, M_t is the torque at time t. [Color figure can be viewed in the online issue, which is available at wileyonlinelibrary.com.]

[eq. (25)] and is labeled in the following text as the single DIFF-EQ model.

COMPARISON OF THE ONE DIFF-EQ MODEL (SINGLE DIFF-EQ MODEL), ODE SYSTEM, AND THE EXPERIMENTAL DATA

To assess the capabilities of the DIFF-EQ model proposed in the reproduction of the experimental EPDM vulcanization process, the experimental data presented in the previous section and conducted within this research program are here reconsidered as reference data.

To perform a numerical optimization of the kinetic model proposed, we normalized the experimental cure values by dividing each point of the curve by the maximum torque values, so that experimental data were always within the range 0–1.

In Figure 7, a comparison between cure curves provided by this approach and the experimental results is sketched for Dutral TER 4049 for a temperature equal to 160°C. Numerical curves were obtained with a nonlinear least-squares procedure, for which the convergence performance of both models is evaluated in Figure 8. In particular, in Figure 8, the difference between the normalized experimental torque and numerical predictions is represented at successive iterations and at increasing instants between the initial and final times of experimentation. Obviously, as expected, when passing from the initial iteration to the final one, such a difference decreased drastically; this means that the least-squares routine achieved convergence. As it is

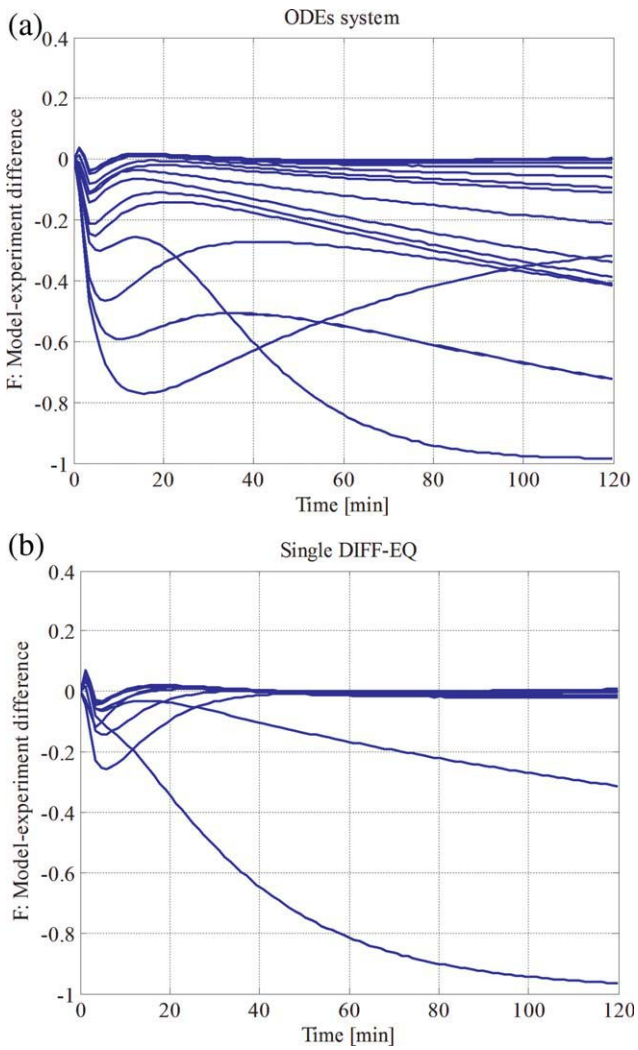

Figure 8 Convergence of the nonlinear least-squares algorithm at successive iterations: (a) ODE system and (b) single DIFF-EQ solution for Dutral TER 4049 at 160°C. F is the difference between normalized torque provided by the model and experimental data. [Color figure can be viewed in the online issue, which is available at wileyonlinelibrary.com.]

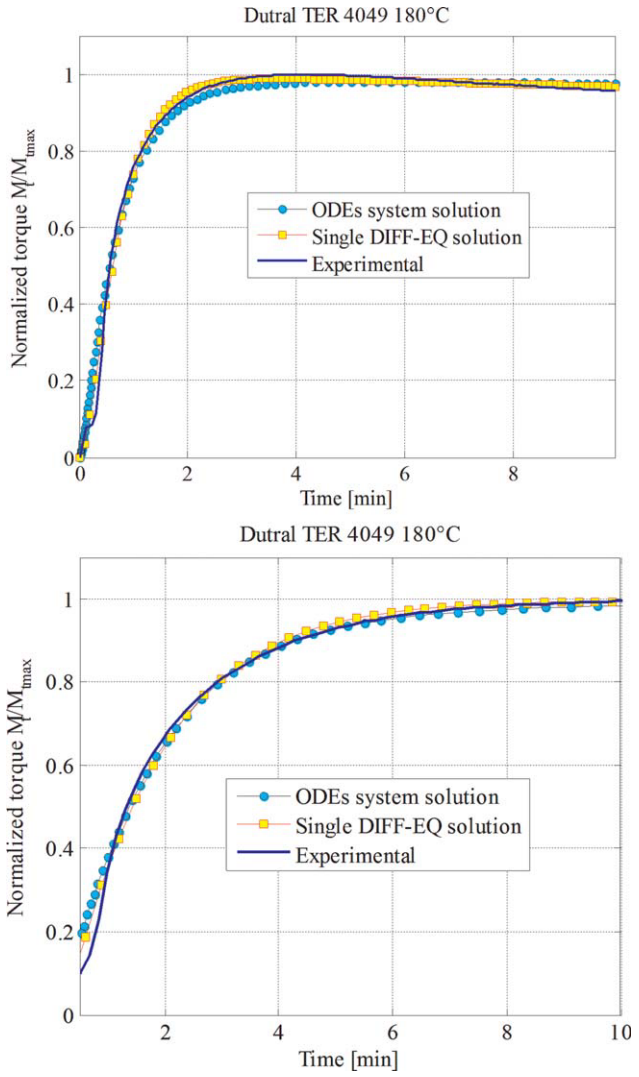

Figure 9 Comparison between the experimental data and the numerical models proposed (bottom: detail after the scorch point) for Dutral TER 4049 at 180°C. [Color figure can be viewed in the online issue, which is available at wileyonlinelibrary.com.]

possible to notice, the gap between the numerical models and experimental data tended toward zero for almost the instants inspected, except for the initial simulation range, immediately before the scorch point. Here, the experimental curve exhibits a sudden increase in the first derivate; this means that the initiation of vulcanization was prone to occur. In any case, this stage is of little interest for the models proposed, which are designed for a reliable prediction of the final reticulation level. From Figure 8, it appears rather clearly that the model based on the single DIFF-EQ converged with the experimental data after a few iterations, whereas the model based on the ODE system approximated the reference solution slowly.

Comparisons at temperatures of 180 and 200°C are replicated in Figures 9 and 10, respectively. Again, the agreement with experimental response seemed rather promising, especially for the single DIFF-EQ model, which seemed to perform slightly better than the first-order system of DIFF-EQs. On the other hand, it is worth noting that for the single DIFF-EQ model, an explicit solution was at our disposal, and therefore, its applicability for practical purposes is much more straightforward.

The blend exhibited a rather marked reversion when vulcanized at 200°C, which is a typical situation for EPDM vulcanized at high temperatures. From an overall analysis of the simulations results, it can be noted that the prediction of the degree of reversion was rather accurate, especially with the single DIFF-EQ model.

The same comparisons performed for Dutral TER 4049 are repeated for Dutral TER 9046 in Figures 11

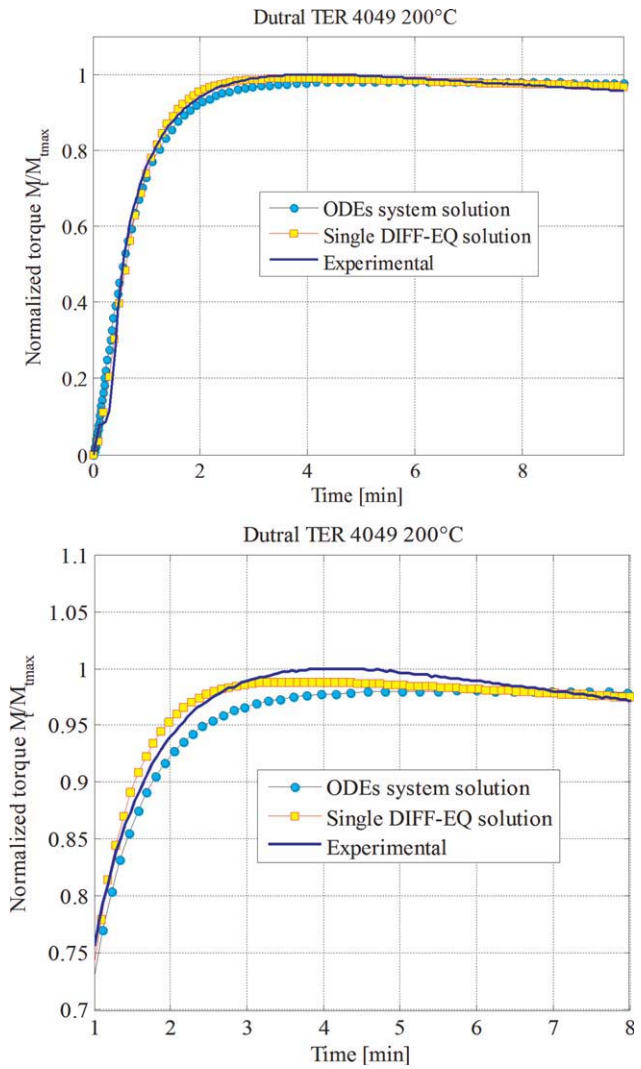

Figure 10 Comparison between the experimental data and the numerical models proposed (bottom: detail after the scorch point) for Dutral TER 4049 at 200°C. [Color figure can be viewed in the online issue, which is available at wileyonlinelibrary.com.]

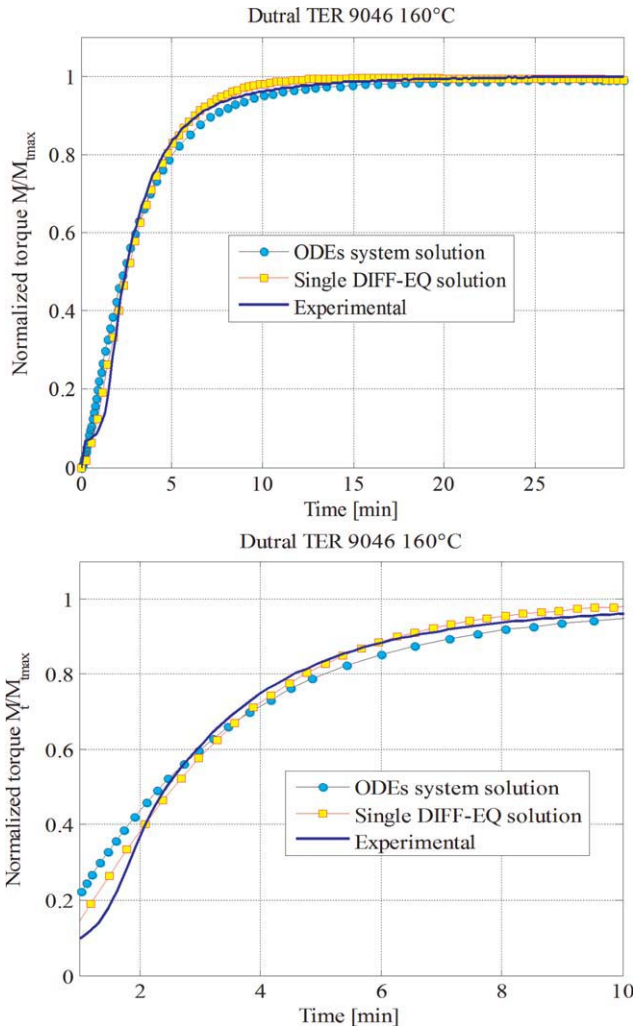

Figure 11 Comparison between the experimental data and the numerical models proposed (bottom: detail after the scorch point) for Dutral TER 9046 at 160°C. [Color figure can be viewed in the online issue, which is available at wileyonlinelibrary.com.]

and 12, respectively, at 160 and 180°C. Also, in this case, the reliability of the numerical model proposed seemed promising, providing results again in satisfactory agreement with the experimental data.

From a comparative analysis of the numerical model performance, it can be noted that almost all of the experimental curves had an induction period before the uprising portion (e.g., Figs. 7 and 8), whereas the curves provided by the model did not exhibit an induction phase. As a result, the fitting deviations were large (Fig. 8) in the very beginning phase. This was not surprising because, before the scorch instant, the model proposed did not hold. At the very beginning, a viscous behavior of the compound was predominant. Then, vulcanization started to occur, and reticulation took place. To be predictive on the first phase, suitable laws linking the viscosity to the viscous stress tensor should be embedded in the model. A non-Newtonian law for the interpretation of the behavior of the compound before scorch is still under study by us and will be presented elsewhere. Here, it is worth emphasizing that simple direct proportionality laws (Newtonian behavior) seem too crude for the interpretation of the problem at hand. Anyway, because the model proposed focuses exclusively on vulcanization issues (after the scorch point), the insufficient fitting in the induction phase was disregarded for the sake of simplicity.

Having at our disposal from the numerical model, in the case of Dutral TER 4049, all three kinetic constants at three temperatures, it was possible to check whether such kinetic constants followed an Arrhenius law with respect to temperature. With this aim, the numerical values were plotted in the Arrhenius space ($1/T$–log K_i plane, with T absolute temperature) to

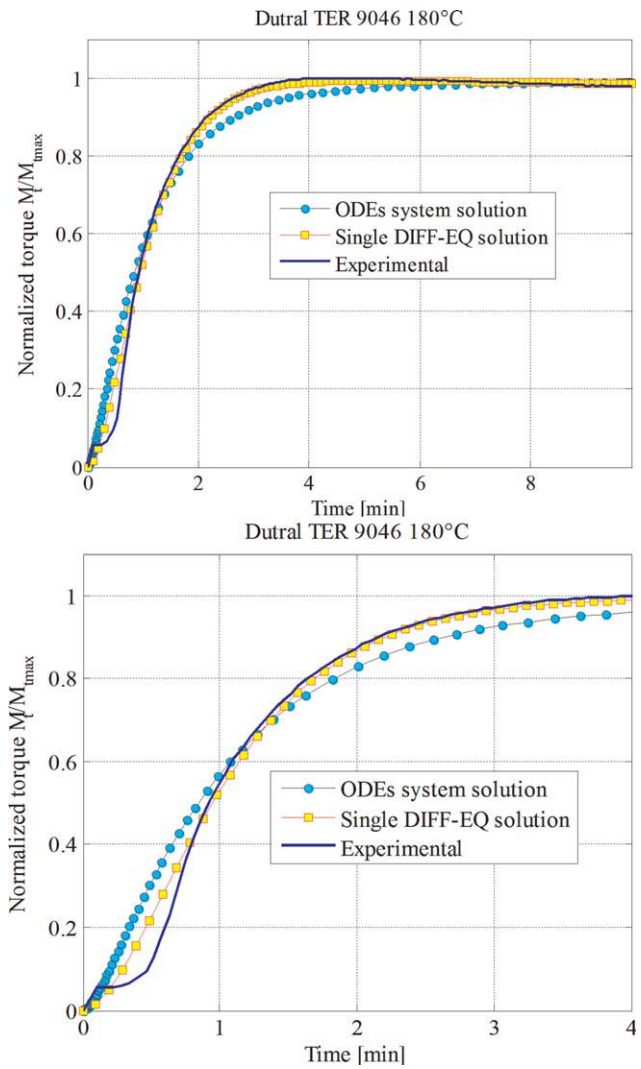

Figure 12 Comparison between the experimental data and the numerical models proposed (bottom: detail at initial vulcanization instants) for Dutral TER 9046 at 180°C. [Color figure can be viewed in the online issue, which is available at wileyonlinelibrary.com.]

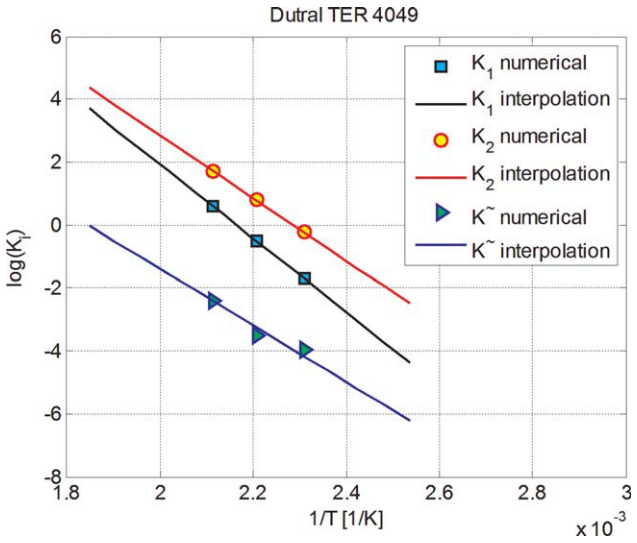

Figure 13 Linear regression interpolation of the kinetic constants provided by the single DIFF-EQ model in the Arrhenius space ($1/T$ – log K_i) for Dutral TER 4049. [Color figure can be viewed in the online issue, which is available at wileyonlinelibrary.com.]

determine whether they were in a straight line. Figure 13 shows, for the three kinetic constants under consideration, the linear regression obtained in the Arrhenius space (squares, circles, and triangles represent the kinetic constants found with the single DIFF-EQ model fit to the experimental data). As it is possible to notice, all three K_i seemed to follow an Arrhenius law of the type $K_i = K_{i0}e^{-E_{ai}/RT}$ rather strictly, where log K_{i0} is defined as the y value of the regression lines in the Arrhenius space for $1/T$ equal to zero (i.e., kinetic constant at infinite temperature), E_{ai}

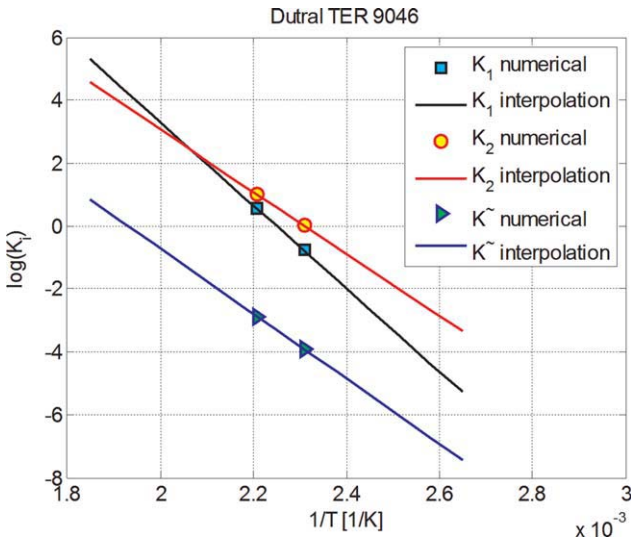

Figure 14 Linear regression interpolation of the kinetic constants provided by the single DIFF-EQ model in the Arrhenius space ($1/T$ – log K_i) for Dutral TER 9046. [Color figure can be viewed in the online issue, which is available at wileyonlinelibrary.com.]

TABLE III
Kinetic Constants and Corresponding E_a's (J/mol) Found with the Single DIFF-EQ Model (Dutral TER 4049)

K_{10} (1 min^{-1} mol^{-1})	K_{20} (1/min)	$\tilde{K}_0$ (1/min)
1.042×10^{11}	7.820×10^{9}	1.525×10^{7}
E_{a1} (J/mol)	E_{a2} (J/mol)	E_a (J/mol)
95,330	81,039	72,921

is the reaction activation energy, and R is the gas constant. In the second case, that is, for Dutral TER 9046, with at our disposal only data for two temperatures, the linear regression obviously passed always for the points found numerically when the experimental data were fitted. The results of the regression are shown in Figure 14.

In Tables III and IV, the kinetic constants K_{i0} and E_{ai} deduced from Figures 13 and 14 are summarized for the first and second compounds analyzed, respectively.

With reference to Figure 15, where a comparison between the three kinetic constants provided by the model for Dutral 9046 and 4049 is reported, the following considerations may be deduced:

1. As expected, the values found for K_1 and K_2 were higher than the values for $\tilde{K}$, which was the combination of the final vulcanization and devulcanization in the entire experimental range and for low EPDM and high insaturation. Although reversion was present at high temperatures for both compounds, obviously, devulcanization is a phenomenon that interests a relatively small amount of crosslinked polymer. Devulcanization sensibly increased with temperature, as correctly predicted by the model (with an increase of $\tilde{K}$). As expected, devulcanization was more critical for Dutral 9046, which exhibited a greater $\tilde{K}$ at high vulcanization temperatures.
2. The observation that K_1 values were systematically higher than $\tilde{K}$ values and generally lower than K_2 values for both EPDMs could be justified by the fact that the reaction between the polymer and the zinc sulfurated complex was very fast and sensitive to temperature variation. Therefore, it is crucial to

TABLE IV
Kinetic Constants and Corresponding E_a's (J/mol) Found with the Single DIFF-EQ Model (Dutral TER 9046)

K_{10} (1 min^{-1} mol^{-1})	K_{20} (1/min)	$\tilde{K}_0$ (1/min)
8.0767×10^{12}	7.8990×10^{9}	4.755×10^{8}
E_{a1} (J/mol)	E_{a2} (J/mol)	E_a (J/mol)
10,7450	80,220	0.84190

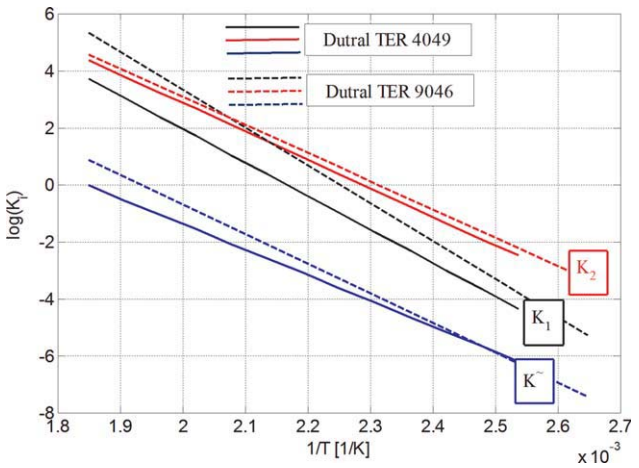

Figure 15 Comparison between kinetic constants of Dutral TER 4049 and 9046. [Color figure can be viewed in the online issue, which is available at wileyonlinelibrary.com.]

homogenize the compounds during the mixing of polymers, filler, accelerators, sulfur, and other additives and coadjuvants.

3. The K_2 values for both EPDMs were quite similar and systematically higher than the K_1 values at low temperatures. This means that the formation of the initial crosslinking was not influenced by small and big amounts of ENB. However, in the EPDM case, the concentration of ENB in terms of double reactive bonds changed from 1 to 2.5 mol %. For other rubber compounds with higher unsaturations, for example, natural rubber and SBR, K_2 values could depend on the concentration of double bonds.
4. $\tilde{K}$ values for both EPDMs were quite similar (with the same order of magnitude), but $\tilde{K}$ found for Dutral 9046 was higher than that found for Dutral 4049, especially at high temperatures. This means that the reversion reaction was more marked in the EPDM with higher unsaturation. It can be stated, therefore, that the reversion was influenced by the amount of reactive double bonds in the macromolecules, that is, by the thermal instability of the sulfur–sulfur bond.

CONCLUDING REMARKS AND FUTURE PERSPECTIVES

In this work, we proposed a mathematical kinetic model for the accelerated curing of EPDM compounds based on best fitting of experimental cure curves provided by a rubber process analyzer (RPA 2000), following the ASTM D 5289 method in the temperature range 160–200°C. We interpreted the reaction mechanism in terms of standard chemical reaction kinetics by means of a second-order nonhomogenous differential model.

For the specific case at hand (EPDM), we are conscious that in the market, a huge amount of polymer types may be encountered, depending on the processes (solution or suspension), the catalyst systems (vanadium compounds, titanium compounds, or metallocenes), and different termonomers used (1,4-hex, dicyclopentadiene, ENB, and vinyl norbornene). Usually, commercial products have different molecular weight distributions, with the ratio between weight-average and number-average molecular weights ranging from 3.0 to 30. For a single type of polymer and a single compound, to estimate the final crosslinking density, in the model, one needs to have at his or her disposal at least an experimental cure curve, successively fitted by a simple function obtained through the closed form solution of a DIFF-EQ.

From the simulation results and experimental data, it can be argued that at high-temperature vulcanization, EPDM with a low unsaturation (i.e., with low weight percentage of ENB) suffers little for reversion. Therefore, the maximum torque maintains its values after the optimal vulcanization time. As a result, it is possible to obtain a good level of vulcanization degree of thick items (where the skin undergoes completely different time–temperature histories with respect to the core). Furthermore, it is possible to increase the productivity of industrial items because the temperature of crosslinking may be increased without the risk of overvulcanizing the items (because reversion is minimal). When an increase of the vulcanization temperature is possible, the time of production decreases. All of these considerations may result in strong cost reduction. For a technological point of view, future perspectives include the production of recyclable items with easy devulcanization and new nitrosamine-free compound recipes. The use of sulfur vulcanization with reduced Zn levels or no Zn at all will be a future issue for both EPDM and other elastomers. Typically, EPDM compounds have aging resistance and faster crosslinking, which can be increased at higher temperatures. A reduction in the ENB amount typically results in a reduction of reversion. All of these considerations could lead to cost reduction of the processes, with invariant performances. Obviously, numerical models, as the one presented in this article, able to furnish predictive information on these crucial issues at very low cost may be of interest for many producers.

References

1. Goodyear, C. U.S. Pat. 3633 (1844).
2. Billmeier, F. W., Jr. Textbook of Polymer Science, 3rd ed.; Wiley: New York, 1984.

3. Krejsa, M. L.; Koenig, J. L. Rubber Chem Technol 1993, 66, 376.
4. Coran, A. Y. In Science and Technology of Rubber; Academic: New York, 1978; Chapter 7.
5. The Chemistry and Physics of Rubber-Like Substances; Bateman, L., Ed.; MacLaren: London, 1963.
6. Rubber Technology, 2nd ed.; Morton, M., Ed.; Van Nostrand Reinhold: New York, 1981.
7. Milani, G.; Milani, F. J Appl Polym Sci 2011, 119, 419.
8. Poh, B. T.; Wong, K. W. J Appl Polym Sci 1998, 69, 1301.
9. Annual Book of ASTM Standards; ASTM D 5289–07; American Society for Testing and Materials: West Conshohocken, PA, 2007.
10. Ding, R.; Leonov, I. J Appl Polym Sci 1996, 61, 455.
11. Jia, Y.; Sun, S.; Liu, L.; Zhong, J. Polym Int 2004, 53, 41.
12. Kosar, V.; Gomzi, Z. Thermochim Acta 2007, 457, 70.
13. Arrillaga, A.; Zaldua, A. M.; Atxurra, R. M.; Farid, A. S. Eur Polym J 2007, 43, 4783.
14. Dispenza, C.; Carter, J. T.; McGrail, P. T.; Spadaro, G. Polym Int 1999, 48, 1229.
15. Chapman, A. V.; Porter, M. In Natural Rubber Science and Technology; Roberts, A. D., Ed.; Oxford University Press: Oxford, England, 1978; Chapter XII.
16. Kresja, M. R.; Koening, J. L. Rubber Chem Technol 1993, 66, 376.
17. Dikland, H. G.; Van Duin, M. In Handbook of Spectroscopy of Rubbery Materials; Rapra Technology: Shropshire, England, 2001.
18. Van Den Berg, J. F. M.; Beulen, J. W.; Duynstee, E. F. J.; Nelissen, H. L. Rubber Chem Technol 1984, 57, 265.
19. Van Den Berg, J. F. M.; Beulen, J. W.; Hacking, J. M. H.; Duynstee, E. F. J. Rubber Chem Technol 1984, 57, 725.
20. Duynstee, E. F. J. Kautsch Gummi Kunstst 1987, 40, 205.
21. Frensdorf, H. K. Rubber Chem Technol 1972, 45, 1348.
22. Winters, R.; Heinen, W.; Verbruggen, M. A. L.; Van Duin, M.; de Groot, H. J. M. Macromolecules 2002, 35, 1958.
23. ASTM D 412–06ae2; Annual Book of ASTM Standards; American Society for Testing and Materials: West Conshohocken, PA, 2006.
24. Tonpheng, B.; Yu, J. C.; Andersson, B. M.; Andersson, O. Macromolecules 2010, 43, 7680.
25. Flory, P. J. Principles of Polymer Chemistry; Cornell University Press: Ithaca, NY, 1953; Chapter XI.
26. Evans, G.; Blackledge, J.; Yardley, P. Numerical Methods for Partial Differential Equations, 2nd ed.; Springer-Verlag: Berlin, 2001.
27. Van Duin, M. Kautsch Gummi Kunstst 2002, 55, 205.
28. Coleman, T. F.; Li, Y. Math Programming 1994, 67(2), 189.
29. Matlab 7.4 User's Guide; MathWorks: Natick, MA, 2007. http://www.mathworks.com/products/matlab/. Accessed on July 15, 2011.